Tetrahedron 74 (2018) 1288–1293

Contents lists available at ScienceDirect

Tetrahedron

journal homepage: www.elsevier.com/locate/tet

Antimicrobial activity of simplified mimics of celogentin C

Varsha J. Thombare [a, b], James A. Holden [b, c], Sreetama Pal [d, e], Eric C. Reynolds [b, c], Amitabha Chattopadhyay [e, f], Neil M. O'Brien-Simpson [b, c], Craig A. Hutton [a, b, *]

[a] School of Chemistry, The University of Melbourne, Victoria 3010, Australia
[b] Bio21 Molecular Science and Biotechnology Institute, The University of Melbourne, Victoria 3010, Australia
[c] Melbourne Dental School and Bio21 Molecular Science and Biotechnology Institute, The University of Melbourne, Victoria 3010, Australia
[d] CSIR-Indian Institute of Chemical Technology, Uppal Road, Hyderabad 500 007, India
[e] Academy of Scientific and Innovative Research, New Delhi, India
[f] CSIR-Centre for Cellular and Molecular Biology, Uppal Road, Hyderabad 500 007, India

ARTICLE INFO

Article history:
Received 4 October 2017
Received in revised form
5 December 2017
Accepted 14 December 2017
Available online 20 December 2017

Keywords:
Celogentin
Antimicrobial peptides
Stapled peptides
Cyclic peptides

ABSTRACT

Linear and bicyclic analogues of the peptide natural product, celogentin C, have been prepared in which the sidechain–sidechain crosslinks in celogentin are omitted or replaced with a mesitylenyl moiety. The simplified bicyclic peptides display moderate antibacterial activity, potentially through inhibition of bacterial protomicrotubule formation, while the linear analogs show higher antibacterial activity through a possible membrane disruption mechanism.

1. Introduction

The development and approval of peptide therapeutics has been steadily increasing over the past two decades, such that >25 peptide therapeutics are now clinically approved, and >140 candidates are undergoing clinical trials.[1–3] Cyclic peptides have shown to be a particularly successful subgroup of therapeutic peptides, with nine cyclic peptides – accounting for 3% of new therapeutics – approved for clinical use from 2006 to 2015.[4–6] Natural product cyclic peptides such as cyclosporine, romidepsin, vancomycin and daptomycin, and more recently their (semi)synthetic derivatives such as telavancin and caspofungin, are valuable drugs employed as antibiotics, antifungals and anti-cancer agents.[4] Cyclic peptides exhibit several properties that lead to their success as clinical therapeutics, including improved binding affinity and selectivity, serum stability and low toxicity.

Though semi-synthetic cyclic peptides have been generated through replacement of long chain acyl groups,[7,8] modifications to the core scaffold of complex cyclic peptide natural products often require total synthesis,[9] which is lengthy and not cost effective. Modifications to introduce stable, non-reducible cross-linkages have been developed in recent years to improve pharmacodynamic properties of peptides.[10–13] Examples of such cross-links include olefins (through cross-metathesis), triazoles (through CuAAC reactions) and thioethers (through alkylation of cysteines with bis- or tris-electrophiles). Aryl and alkyl halides are most commonly employed in cysteine cross-linking reactions, in addition to acrylamide/maleimide Michael-type acceptors. Notably, the groups of Timmerman and Heinis have employed a one-step process for the cross-linking of linear peptides containing three cysteine residues upon treatment with tris-(bromomethyl)benzene (TBMB), to generate constrained bicyclic adducts containing three thioethers.[14–17] This approach has been employed to generate large, phage-encoded libraries of bicyclic peptides, which combined with iterative affinity selection has facilitated the discovery of numerous biologically active peptides.[18–20]

Cross-linked aromatic amino acids occur commonly in bicyclic peptide natural products, wherein covalent links between the aromatic side chain and other amino acid sidechains generates a central aromatic core. Examples include the central phenylglycine residue in vancomycin and the tryptophan residue in phalloidin and celogentin (Fig. 1).[21–23] Such peptide natural products possess

* Corresponding author. School of Chemistry, The University of Melbourne, Victoria 3010, Australia.
E-mail address: chutton@unimelb.edu.au (C.A. Hutton).

https://doi.org/10.1016/j.tet.2017.12.032
0040-4020/

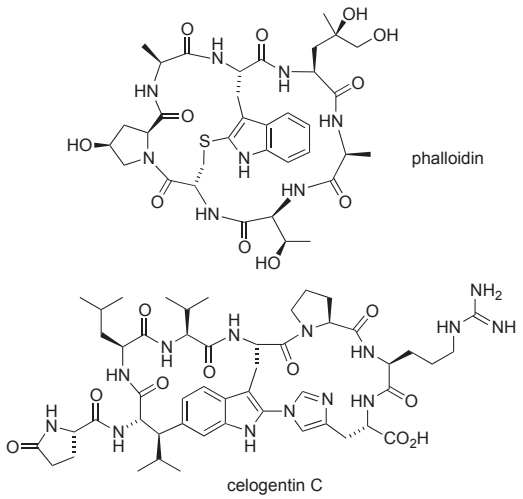

Fig. 1. Cross-linked cyclic peptides phalloidin and celogentin C.

diverse biological activities, including anti-tumour and antibacterial properties. The total synthesis of, for example, celogentin C has been completed by several groups, and requires at least 19 steps in lengthy, complex synthetic routes.[24–27]

We postulate that analogues of bicyclic peptide natural products, such as the celogentins or phalloidin, could be generated by replacing the central aromatic core with aromatic moieties more routinely employed as stapling groups. Such bioinspired bicyclic peptides should be much more synthetically accessible than the natural products themselves, and more amenable to the generation of libraries of analogues to assess structure–activity relationships and fine-tune biological properties. Though such aromatic linkers have been used to install conformational constraints in linear peptides, to the best of our knowledge such cross-linking agents have not been employed as replacements for the core scaffold of naturally occurring cyclic peptides. We chose celogentin C as the starting point for our investigations as the indole of the central tryptophan residue is connected to three side-chains and is therefore suitable for replacement by a triple thioether-linked core, and the remaining residues are all easily accessible proteinogenic amino acids.

2. Results and discussion

2.1. Design and synthesis

The design of simplified celogentin C analogues was based on substitution of the three native cross-linked amino acid residues –leucine, tryptophan and histidine– with three cysteine residues. Cross-linking of the three cysteine residues with TBMB would then generate a celogentin C analogue with the central indole core replaced with a 1,3,5-trisubstituted benzene core.

The corresponding linear peptide, ZCLVCPRC, was synthesized on chlorotrityl resin using standard SPPS techniques. The unprotected linear peptide was treated with TCEP in buffer overnight to ensure the cysteine residues were reduced, then the peptide solution was treated with TBMB to generate the bicyclic peptide (Scheme 1). To optimize the reaction conditions for conjugation, the conjugation reaction was performed using five different buffer systems (TRIS buffer, pH7.4; guanidium buffer, pH 5.5 and 8.5; phosphate buffer, pH7.4; triethanolamine (TEA) buffer, pH8.2, and; ammonium bicarbonate buffer, pH 8). Each reaction was monitored by HPLC and mass spectrometry at 5 min, 1 h, 6 h, 12 h and 24 h. The bicyclic peptide was formed only in ammonium bicarbonate and TEA buffers. Ammonium bicarbonate buffer was found to be most efficient, with complete consumption of linear peptide observed within 1 h (Fig. S1, supporting information). These optimized conditions (ammonium bicarbonate buffer, pH 8.0, 1 h) were then employed for the synthesis of all analogues.

To determine the role of amino acid side chains, a range of peptides were designed through an alanine scan, with each (non-Cys) residue replaced successively with Ala. Pyroglutamate was replace with N-Ac-Ala. The linear peptides were synthesized with both acid and amide C-termini using chlorotrityl and Rink-amide resins, respectively (Table 1). Each linear peptide was treated with TBMB to yield the corresponding bicyclic adduct (Table 2). Interestingly, reactions of the C-terminal amide peptides with TBMB proceeded significantly faster to generate the corresponding bicyclic adducts in higher yields than reactions of the peptides possessing C-terminal acids. Further, linear peptide acid **1c** failed to produce a bicyclic peptide upon treatment with TBMB. The bicyclic peptides were purified by HPLC (see supporting information).

All linear and bicyclic peptides were characterized by ESI mass spectrometry, displaying characteristic *m/z* peaks corresponding to $M+H^+$ or $M+2H^+$ ions. Furthermore, bicyclic peptide **2a** was characterized by 1D and 2D NMR spectroscopy (COSY) (see supporting information).

2.2. Antimicrobial assays

The synthesized analogues **2a**–**2g**, **4a**–**4g**, **5** and **6** were assayed for activity against Gram-positive *Staphylococcus aureus* and Gram-negative *Escherichia coli* strains. Antimicrobial assays to determine minimal inhibitory concentration (MIC) and minimal bactericidal concentration (MBC) were conducted against a Gram-positive and Gram-negative bacterial strains, *Staphylococcus aureus* and *Escherichia coli*, respectively, using methods previously described.[28] None of the peptide analogues displayed significant bactericidal activity against either bacteria or inhibitory activity against *S. aureus*. However, analogues **5**, **6**, **4a** and **4d** did exhibit moderate inhibitory activity against *E. coli* (Table 3). Intriguingly, linear regression analysis of the exponential growth phase found that there was significant differences in the rate of growth compared to control for *E. coli* grown in the presence of analogues **5** ($F(1, 20) = 18.78$, $p = .0003$, $R^2 = 0.99$), **6** ($F(1, 20) = 70.72$, $p < .0001$, $R^2 = 0.99$), and bicyclic analogue **4a** ($F(1, 20) = 14.25$, $p = .0012$, $R^2 = 0.98$). Further, peptides **5**, **6**, **4a** and **4d** significantly ($p < .01$) reduced the biomass of *E. coli* compared to control at the point of stationary phase (350 min incubation) and eliminated the slow growth rate typically seen during the stationary phase (Fig. 2). The bicyclic peptide amides **4a** and **4d** displayed moderate inhibition of *E. coli* growth, while the linear peptide amide **6** was the most active compound (Fig. 3). The reduction of the growth rate and biomass of *E. coli* by the celogentin mimic **4a** may be a result of anti-mitotic (anti-binary fission) activity. Celogentin C's mode of action in preventing eukaryote cell division is by inhibiting tubulin polymerization; bacteria have tubulin homologues for cytokinesis and inhibitors of polymerization of such tubulin homologues have been shown to reduce bacterial growth rates and biomass.[29]

Linear peptides **5** and **6**, which displayed the highest antibacterial activity, may have an alternative mode of action and could be exerting their effect through membrane binding interactions, as is commonly observed for other linear antimicrobial peptides (AMPs),[30] rather than as celogentin C mimics.[31] Accordingly, we next pursued studies of the interaction of the most active peptides, **5** and **6**, with model membrane systems.

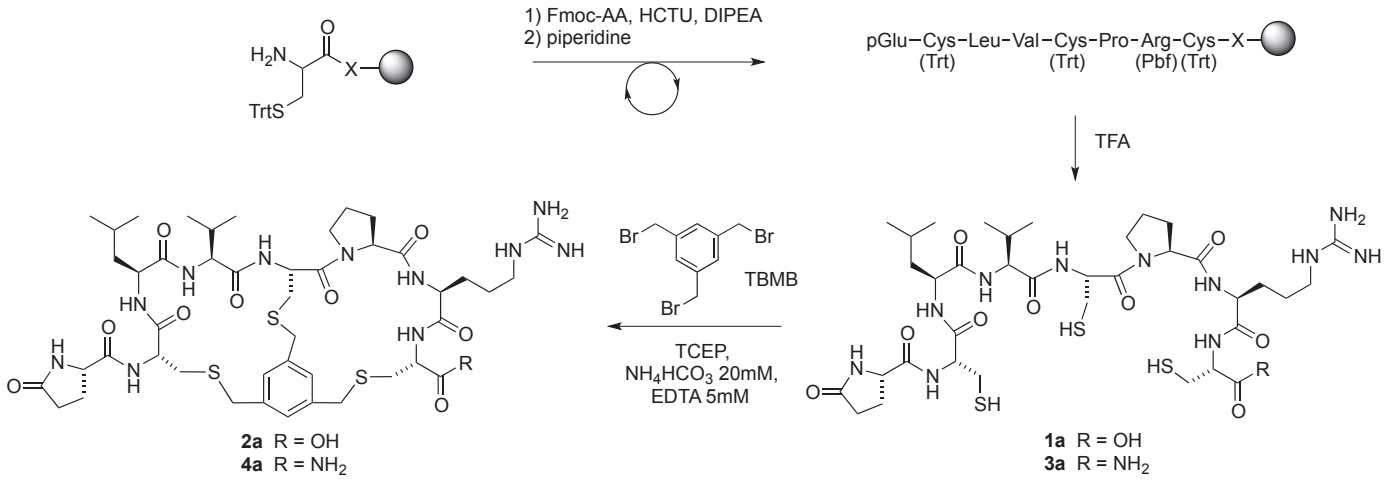

Scheme 1. Synthesis of bicyclic peptide adducts.

Table 1
Linear peptide sequences (isolated yields in parentheses).

Sequence[a]	Comp.	Yield %
ZCLVCPRC–OH	**1a**	58
ZCLVCPAC–OH	**1b**	47
ZCLVCARC-OH	**1c**	52
ZCLACPRC–OH	**1d**	55
ZCAVCPRC–OH	**1e**	56
Ac–ACLVCPRC–OH	**1f**	62
ZCLVCGRC–OH	**1g**	48
ZCLVCPRC–NH_2	**3a**	66
ZCLVCPAC–NH_2	**3b**	60
ZCLVCARC–NH_2	**3c**	58
ZCLACPRC–NH_2	**3d**	60
ZCAVCPRC–NH_2	**3e**	61
ACLVCPRC–NH_2	**3f**	64
ZCLVCGRC–NH_2	**3g**	62
ZLLVWPRH–OH	**5**	63
ZLLVWPRH–NH_2	**6**	66

[a] Z = pyroglutamyl.

Table 2
Cyclic peptide sequences (isolated yields in parentheses).

Sequence[a,b]	Comp.	Yield %
ZC*LVC*PRC*–OH	**2a**	46
ZC*LVC*PAC*–OH	**2b**	40
ZC*LAC*PRC*–OH	**2d**	42
ZC*AVC*PRC*–OH	**2e**	57
Ac–AC*LVC*PRC*–OH	**2f**	44
ZC*LVC*GRC*-OH	**2g**	45
ZC*LVC*PRC*–NH_2	**4a**	65
ZC*LVC*PAC*–NH_2	**4b**	65
ZC*LVC*ARC*–NH_2	**4c**	60
ZC*LAC*PRC*–NH_2	**4d**	64
ZC*AVC*PRC*–NH_2	**4e**	63
AC*LVC*PRC*–NH_2	**4f**	64
ZC*LVC*GRC*–NH_2	**4g**	62

[a] Z = pyroglutamyl.
[b] C* = Cys connected through 1,3,5-trismethylenylbenzene.

Table 3
Antimicrobial assays; MIC (μM).

Peptide	Bacterial strain	
	S. aureus	*E. coli*
Aurein	18.7	36.5
Vancomycin	2.5	4.5
5	>500	388
6	>500	292
2a	>500	>500
2b	>500	>500
2c	>500	>500
2d	>500	>500
2e	>500	>500
4a	>500	419
4b	>500	>500
4c	>500	>500
4d	>500	442
4e	>500	>500

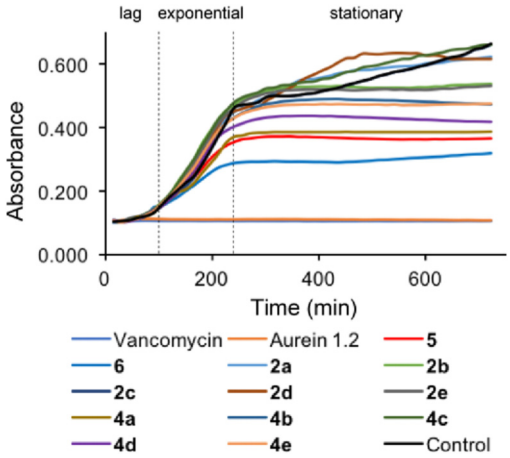

Fig. 2. *E. coli* growth curve in presence of peptides **5**, **6**, **2a**–**2e**, **4a**–**4e** (at 110 μM), vancomycin (3.4 μM) and aurein1.2 (55 μM), showing lag, exponential and stationary phases.

2.3. Membrane binding assays

Binding studies of linear peptides **5** and **6** (possessing C-terminal acid and amide functionality, respectively) with model membranes composed of POPC, POPC/POPG (80/20, mol/mol), POPE/POPG (80/20, mol/mol) or POPG/CL (50/50, mol/mol) were explored in an attempt to understand if the differential bacterial uptake of these two peptides were linked to their affinity to bacterial membranes. Gram-positive and Gram-negative bacterial (inner) membranes were mimicked by LUVs containing binary mixtures of

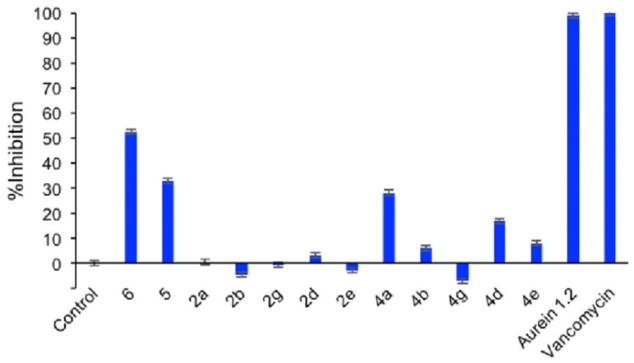

Fig. 3. Inhibition of *E. coli* growth by peptides **5**, **6**, **2a**–**2e**, **4a**–**4e** (at 110 μM), vancomycin (3.4 μM) and aurein1.2 (55 μM). The percent inhibition was determined at 310 min of growth (entry of stationary phase). Data is represented as the mean ± SD of 3 biological replicates.

POPE/POPG (80/20) and POPG/CL (50/50).[32] The effect of negatively charged POPG was explored since negatively charged lipids are known to be critical for the proper insertion/adsorption, folding and function of numerous membrane-interacting proteins.[33–35]

Binding of the amidated peptide **6** to membranes appears to be tighter, relative to the acid analog **5**, as indicated by the greater increase in normalized fluorescence intensity from the tryptophan of the amide analog in the presence of lipid vesicles (Fig. 4). This trend was observed across all four lipid compositions studied. However, none of the binding isotherms could be fitted to a single-site binding model (given by a simple hyperbolic function), indicating that the overall membrane affinity of the peptides is not high. Moreover, the shift in the emission maximum of tryptophan in the presence of membranes peptides was small (~2 nm, see Fig. S8).

However, changes in tryptophan fluorescence reports solely on local changes in the microenvironment of the centrally located tryptophan residue in the peptide and may not be representative of the global changes induced in the membrane due to interaction with the peptides. Therefore, we complemented the tryptophan binding experiments with studies that monitor changes in fluorescence of the lipophilic, potential sensitive fluorophore, di-8-ANEPPS in the presence of the celogentin analogs. Di-8-ANEPPS reports on the membrane dipole potential, which is the potential difference within the membrane bilayers originating due to the nonrandom arrangement of molecular dipoles corresponding to the lipid carbonyls and water molecules at the membrane interface.[36–38] Dipole potential has been previously reported to be a sensitive tool to explore membrane interaction of peptides.[34,39]

The differences in membrane binding among the two analogs emerge clearer once the fluorescence difference spectra of di-8-ANEPPS for the two analogs are compared (Fig. 5). The fluorescence signature of di-8-ANEPPS in the presence of the amidated peptide **6** shows an appreciable increase, relative to that in the presence of the acid analog, across all four membrane systems. The increase in fluorescence can be attributed to greater membrane affinity of the amide analog **6** and this may contribute to the greater bactericidal properties of the analog **6**.

In conclusion, we have synthesized a family of analogues of the peptide natural product, celogentin C, in which the cross-linked aromatic core is replaced with a 1,3,5-trisubstituted benzene moiety, or in which the sidechain–sidechain crosslinks have been omitted. The peptides displayed moderate antibacterial activity against Gram-positive *E. coli* but not against Gram negative *S. aureus*. The simplified bicyclic analogues displayed antibacterial activity consistent with inhibition of bacterial protomicrotubule formation. Further, the linear amidated peptide **6** displayed comparatively higher membrane affinity, relative to the acid analogue **5**, and this indicates that the antibacterial activity could be consistent with a membrane disruption mechanism.

3. Experimental

3.1. Materials

DMPC (1,2-dimyristoyl-*sn*-glycero-3-phosphocholine), POPC (1-palmitoyl-2-oleoyl-*sn*-glycero-3-phosphocholine), POPG (1-palmitoyl-2-oleoyl-*sn*-glycero-3-phosphatidylglycerol), POPE (1-palmitoyl-2-oleoyl-*sn*-glycero-3-phosphoethanolamine) and CL

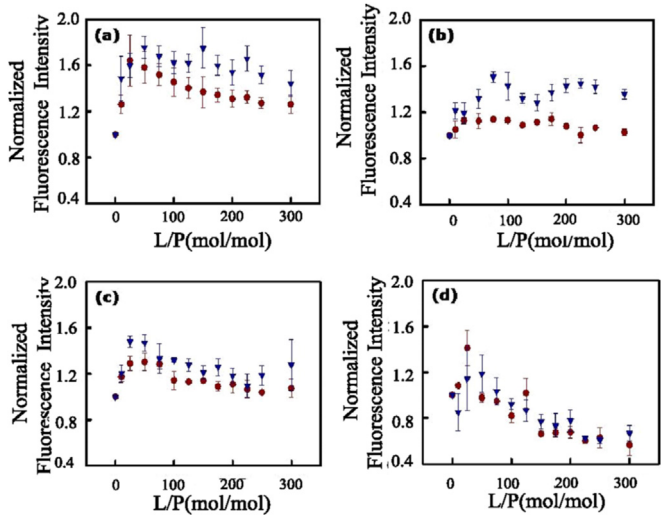

Fig. 4. Change in tryptophan fluorescence intensity at the respective emission maximum in LUVs of (a) POPC, (b) POPC/POPG (80/20, mol/mol), (c) POPE/POPG (80/20, mol/mol) and (d) POPG/CL (50/50, mol/mol) with increasing lipid-to-peptide (L/P) ratio of the peptide acid **5** (●) and amide **6** (▼). Normalized fluorescence intensity is representative of ≥3 replicates. Excitation wavelength 280 nm, [peptide] = 2 μM.

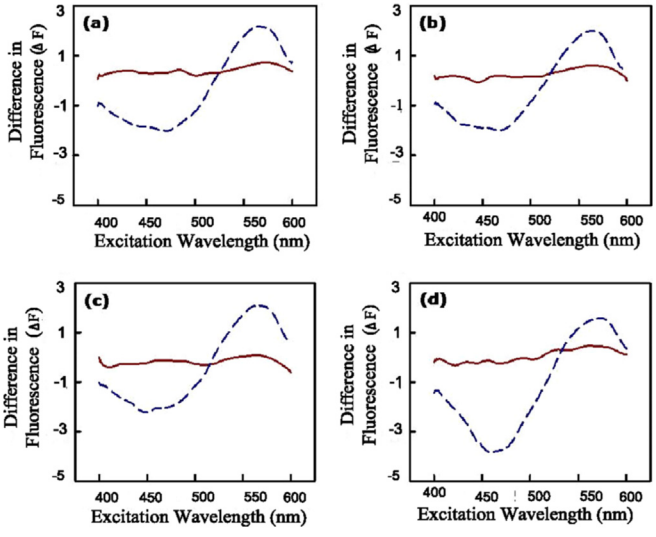

Fig. 5. Fluorescence difference spectra of the potential-sensitive fluorophore, di-8-ANEPPS, in LUVs of (a) POPC, (b) POPC/POPG (80/20, mol/mol), (c) POPE/POPG (80/20, mol/mol) and (d) POPG/CL (50/50, mol/mol) in the presence of **5** (solid line, ——) and **6** (dashed line, – – –). Emission wavelength 670 nm, [peptide] = 20 μM, L/P ratio = 10:1.

(cardiolipin from bovine heart, disodium salt) were obtained from Avanti Polar Lipids (Alabaster, AL). di-8-ANEPPS was purchased from Molecular Probes/Invitrogen (Eugene, OR). Sodium phosphate and sodium chloride were obtained from Sigma Chemical Co. (St. Louis, MO). Lipids were checked for purity by thin layer chromatography on silica gel pre-coated plates obtained from Merck (Darmstadt, Germany) in chloroform/methanol/water (65:35:5, v/v/v) and were found to give a single spot in all cases when visualized upon charring with a solution containing cupric sulfate (10%, w/v) and phosphoric acid (8%, v/v) at 150 °C.[40] The concentrations of phospholipids were determined by phosphate assay subsequent to total digestion by perchloric acid.[41] DMPC was used as an internal standard to assess lipid digestion. All other chemicals used were of the highest purity available. Solvents used were of spectroscopic grade. Water was purified through a Millipore (Bedford, MA) Milli-Q system and used throughout. Concentrations of stock solutions of di-8-ANEPPS in methanol was estimated from its molar extinction coefficient (ε) of 37,000 M^{-1} cm^{-1} at 498 nm.[42] The concentration of the peptides in water was estimated using the molar extinction coefficient (ε) of 5570 M^{-1} cm^{-1} at 280 nm for the sole tryptophan.[33]

3.2. General protocol for solid phase peptide synthesis

The linear peptides were synthesized using standard Fmoc SPPS coupling methods on-resin with the C-terminal acid (Wang/chlorotrityl resin) and amide (Rink amide resin). The coupling steps were performed using a CEM Liberty Blue microwave peptide synthesizer. All peptides were synthesized on 0.1 mmol scale using a 4 or 5-fold molar excess of Fmoc-protected amino acid (0.4 or 0.5 mmol for a 0.1 mmol scale) that were activated using a 4- or 5-fold excess of HCTU in the presence of DIEA (8–10 equivalents). The Fmoc deprotection was performed with 20% v/v piperidine in DMF.

3.3. Cleavage of peptide from solid support

After completion of solid phase synthesis, the peptides were cleaved from the solid support by treatment with a cleavage cocktail of trifluoroacetic acid (TFA):triisopropylsilane (TIPS):3,6-dioxa-1,8-octanedithiol (DODT):water (94:2.5:2.5:1, 15 mL/0.1 mmol of peptide) for 2 h. The cleavage cocktail was evaporated under nitrogen and the remaining residue was precipitated with ice-cold diethyl ether and centrifuged at 3000 rpm for 3–5 min. Pellets were washed three times by resuspending in ice-cold diethyl ether followed by centrifugation.

3.4. Purification

Peptide purification was performed using an Agilent RP-HPLC with a C18 Phenomenex 250 × 10 mm, 2 μ column. The peptide purity was assessed using a C18 Phenomenex 150 × 4.6 mm, 5 μ column in a gradient mode with eluent (buffer) A; 0.1% aq. TFAand buffer B; 0.1% TFA in acetonitrile. RP-HPLC was performed using gradient elution with buffer B 0–40% over 40min, monitoring at a wavelength of 214 nm.

3.5. Characterization of peptides

All synthesized peptides were characterized by LC-MS (Agilent or ThermoXcalibar).

3.6. Peptide cross-linking

Buffer: Ammonium bicarbonate (79.06 mg) and EDTA (93 mg) were dissolved in 50 mL milliQ water and the solution pH was adjusted to 8 with 0.1 M HCl. Linear peptide (2 mg, 2.132 μmol) was dissolved in aq. ammonium bicarbonate buffer (10 mL) and tris(2-carboxyethyl)phosphine (TCEP) (0.640 mg, 2.56 μmol) was added in peptide and stirred overnight.1,3,5-tris(bromomethyl)-benzene (1.902 mg, 5.33 μmol) was dissolved in acetonitrile (2 mL). The solution was added to the peptide solution and stirred at room temperature for 3 h, the desired peptide was directly purified by HPLC.

3.7. Antibacterial assays

Antibacterial assays were undertaken to determine the minimum inhibitory concentration (MIC), *E. coli* ATCC 29222 and *S. aureus* ATCC 29213, were grown and maintained at 37 °C on Lysogeny Broth (LB) agar plates. Single colonies from the agar plates were used to inoculate LB and the growth was monitored at 650 nm using a spectrophotometer (model 275E; Perkin-Elmer, Sydney, NSW) with culture purity checked by microscopic examination and culture. Batch-grown cells were harvested during late exponential growth phase and counted using a Quanta SC-MPL flow-cytometer (Beckman Coulter Pty Ltd, Sydney, NSW). For each bacterial strain assays were repeated in a stock solution (2.5×10^5 cells mL^{-1}) in LB media.

All peptides were dissolved in DMSO and a 500 μM stock solution prepared by adding the LB media (final assay concentration of DMSO was ≤2.5% v/v) and serial dilutions (250–0.244 μM) of the peptides in media (100 μl/well) made just prior addition of bacteria. The 100 μl aliquots of the bacterial stock solution (2.5×10^5 cells/well) were added to the peptide a serial dilution and incubated at 37 °C for 90 min. Bacteria were also incubated in the absence of peptide to serve as a growth control for the assay. After the 90min incubation period the antimicrobial activity MIC was determined as follows;

For the determination of MIC after the 90 min incubation, bacterial growth was monitored at 20 min intervals over a 12 or 24 h period by optical density at 620 nm (OD620) using an iEMS microplate reader (Pathtech Pty Ltd, Melbourne, Vic.). The relative growth at each peptide concentration was compared with maximal growth (determined as the point when bacteria incubated in media alone entered the stationary phase of growth, 100% growth), and the MIC was determined as the lowest peptide concentration needed to completely inhibit the growth of the bacteria.

3.8. Sample preparation for membrane binding experiments

All experiments were performed using large unilamellar vesicles (LUVs) of ~100 nm diameter of POPC, POPC/POPG (80/20, mol/mol), POPE/POPG (80/20, mol/mol) or POPG/CL (50/50, mol/mol). Peptide concentration was kept constant at 2 μM, while the lipid concentration ranged from 20 to 600 μM (and therefore, a lipid-to-peptide molar ratio of 10–300) for binding experiments utilizing tryptophan fluorescence. In experiments utilizing the lipophilic probe di-8-ANEPPS, the total lipid and probe concentrations were 200 and 20 μM, respectively (*i.e.*, the lipid-to-probe molar ratio was 10:1).

For LUV preparation, lipids (POPC or POPC/POPG or POPE/POPG or POPG/CL) were mixed well (in case of binary systems) and dried under a stream of nitrogen while being warmed gently (~35 °C). After further drying under a high vacuum for at least 3 h, the lipid mixture was hydrated (swelled) by addition of 10 mM sodium phosphate, 150 mM sodium chloride, pH 7.2 buffer, and each sample was vortexed intermittently for 3 min to uniformly disperse the lipids to form homogeneous multilamellar vesicles. LUVs of ~100 nm diameter were prepared by the extrusion technique using an Avanti Liposofast Extruder (Avanti Polar Lipids, Alabama, AL) as

previously described.[43] Briefly, the multilamellar vesicles were freeze-thawed five times using liquid nitrogen to ensure solute equilibration between trapped and bulk solutions and then extruded through polycarbonate filters (pore diameter of 100 nm) mounted in an extruder fitted with Hamilton syringes (Hamilton Company, Reno, NV). Samples were subjected to at least 11 passes through the polycarbonate filters to give the final LUV suspension. Background samples for experiments were prepared the same way except that no peptide (or probe) was added. Peptide was incorporated into samples from an aqueous stock solution, followed by an incubation period of 12 h in dark at room temperature (~23 °C). This was done to ensure equilibration of the peptide-membrane system prior to fluorescence data acquisition.

3.9. Membrane binding studies utilizing tryptophan fluorescence

Steady state fluorescence measurements were performed with a Hitachi F-7000 spectrofluorometer (Tokyo, Japan) using 1 cm path length quartz cuvette. Excitation and emission slits with slit widths of 2.5 and 5 nm, respectively, were used for all measurements. All spectra were recorded in the corrected spectrum mode. Background intensities of samples in which the peptide was omitted were negligible in most cases and were subtracted from each sample spectrum to cancel out any contribution due to the solvent Raman peak and other scattering artifacts. Fluorescence intensity at the respective emission maximum of each sample was normalized to that of the peptide in buffer. The normalized fluorescence intensity values were plotted as a function of lipid-to-peptide molar ratio to explore the relative changes in binding affinity of the two analogs. Data shown are representative of at least three independent measurements.

3.10. Membrane binding studies utilizing di-8-ANEPPS fluorescence

Fluorescence excitation spectra were recorded using a Hitachi F-7000 spectrofluorometer (Tokyo, Japan) with 1 cm path length quartz cuvette. Emission wavelength was fixed at 670 nm. Excitation and emission slits with a nominal bandpass of 2.5 nm were used for all measurements. All spectra were recorded in the corrected spectrum mode. Background intensities of samples were subtracted from each sample to cancel any contribution due to the solvent Raman peak and other scattering artifacts. The choice of the emission wavelength (670 nm) at the red edge of the spectrum has previously been shown to rule out the membrane fluidity effects.[44] Fluorescence difference spectra were obtained by subtracting the corrected excitation spectra of samples lacking the peptide from the corrected excitation spectra of samples containing each of the peptide analogs at a lipid-to-peptide molar ratio of 10:1.

3.11. Data analysis and plotting

The fluorescence difference spectra were subjected to a moderate degree of smoothening by the adjacent averaging program available in Microcal Origin version 8.0 (OriginLab, Northampton, MA), while ensuring that the overall spectral shape remains unaltered. Data plots were generated with Sigmaplot version 11.0 (Systat Software Inc., San Jose, CA).

Acknowledgments

This work was supported by the Australian Research Council, The University of Melbourne (IRRTF, MRS to V.T.) and the Council of Scientific and Industrial Research, Govt. of India (A.C.). S.P. thanks the University Grants Commission (Govt. of India) for the award of a Senior Research Fellowship. A.C. is an Adjunct Professor of Tata Institute of Fundamental Research (Mumbai), RMIT University (Melbourne, Australia), Indian Institute of Technology (Kanpur), and Indian Institute of Science Education and Research (Mohali). A.C. gratefully acknowledges support from J.C. Bose Fellowship (Department of Science and Technology, Govt. of India).

Appendix A. Supplementary data

Supplementary data related to this article can be found at https://doi.org/10.1016/j.tet.2017.12.032.

References

1. Kaspar AA, Reichert JM. *Drug Discov Today*. 2013;18:807–817.
2. Fosgerau K, Hoffmann T. *Drug Discov Today*. 2015;20:122–128.
3. Bray BL. *Nat Rev Drug Discov*. 2003;2:587–593.
4. Zorzi A, Deyle K, Heinis C. *Curr Opin Cell Biol*. 2017;38:24–29.
5. Thapa P, Espiritu MJ, Cabalteja C, Bingham J-P. *Int J Pept Res Therapeut*. 2014;20:545–551.
6. Joo S-H. *Biomol Ther*. 2012;20:19–26.
7. Onishi J, Meinz M, Thompson J, et al. *Antimicrob Agents Chemother*. 2000;44:368–377.
8. Goldstein EJC, Citron DM, Merriam CV, Warren Y, Tyrrell K, Fernandez HT. *Antimicrob Agents Chemother*. 2003;47:1968–1971.
9. Okano A, Nakayama A, Schammel AW, Boger DL. *J Am Chem Soc*. 2014;136:13522–13525.
10. Van Arnum P. *Pharm Tech*. 2013;37:48–50.
11. Walensky LD, Bird GH. *J Med Chem*. 2014;57:6275–6288.
12. Lau YH, de Andrade P, Wu Y, Spring DR. *Chem Soc Rev*. 2014;44:91–102.
13. Fairlie DP, Dantas de Araujo A. *Biopolymers*. 2016;106:843–852.
14. Timmerman P, Beld J, Puijk WC, Meloen RH. *ChemBioChem*. 2005;6:821–824.
15. Heinis C, Rutherford T, Freund S, Winter G. *Nat Chem Biol*. 2009;5:502–507.
16. Chen S, Morales-Sanfrutos J, Angelini A, Cutting B, Heinis C. *ChemBioChem*. 2012;13:1032–1038.
17. Rebollo IR, Angelini A, Heinis C. *MedChemComm*. 2013;4:145–150.
18. Wallbrecher R, Depre L, Verdurmen WP, et al. *Bioconj Chem*. 2014;25:955–964.
19. Bertoldo D, Khan MM, Dessen P, Held W, Huelsken J, Heinis C. *ChemMedChem*. 2016;11:834–839.
20. Deyle K, Kong X-D, Heinis C. *Acc Chem Res*. 2017;50:1866–1874.
21. Nolan EM, Walsh CT. *ChemBioChem*. 2009;10:34–53.
22. Yuen AKL, Hutton CA. *Nat Prod Commun*. 2006;1:907–913.
23. Feliu L, Planas M. *Int J Pept Res Therapeut*. 2005;11:53–97.
24. Ma B, Litvinov DN, He L, Banerjee B, Castle SL. *Angew Chem Int Ed*. 2009;48:6104–6107.
25. Feng Y, Chen G. *Angew Chem Int Ed*. 2010;49:958–961.
26. Hu W, Zhang F, Xu Z, Liu Q, Cui Y, Jia Y. *Org Lett*. 2010;12:956–959.
27. Tang J, He Y, Chen H, Sheng W, Wang H. *Chem Sci*. 2017;8:4565–4570.
28. O'Brien-Simpson NM, Pantarat N, Attard TJ, Walsh KA, Reynolds EC. *PLos One*. 2016;11, e0151694.
29. Mathew B, Hobrath JV, Ross L, et al. *PLos One*. 2016;11, e0164100.
30. Lee T-H, Hall K, Aguilar M-I. *Curr Top Med Chem*. 2015;16:25–39.
31. Okpako E, Ajibesin KK. *Am J Res Commun*. 2015;3:123–133.
32. Epand RF, Savage PB, Epand RM. *Biochim Biophys Acta*. 2007;1768:2500–2509.
33. Ghosh AK, Rukmini R, Chattopadhyay A. *Biochemistry*. 1997;36:14291–14305.
34. Chaudhuri A, Chattopadhyay A. *Biochim Biophys Acta*. 2014;1838:2078–2086.
35. Resh MD. *Cell*. 1994;76:411–413.
36. Gross E, Bedlack Jr RS, Loew LM. *Biophys J*. 1994;67:208–216.
37. Clarke RJ. *Adv Colloid Interface Sci*. 2001;89–90:263–281.
38. Haldar S, Kanaparthi RK, Samanta A, Chattopadhyay A. *Biophys J*. 2012;102:1561–1569.
39. Matos PM, Castanho MARB, Santos NC. *PLos One*. 2010;5:e9830.
40. Baron CB, Coburn RF. *J Liq Chromatogr*. 1984;7:2793–2801.
41. McClare CWF. *Anal Biochem*. 1971;39:527–530.
42. Le Goff G, Vitha MF, Clarke RJ. *Biochim Biophys Acta*. 2007;1768:562–570.
43. MacDonald RC, MacDonald RI, Menco BP, Takeshita K, Subbarao NK, Hu LR. *Biochim Biophys Acta*. 1991;1061:297–303.
44. Clarke RJ, Kane DJ. *Biochim Biophys Acta*. 1997;1323:223–239.